IMPROVED HOT-PARTICLE DETECTION AND ISOTOPE SEPARATION WITH REAL-TIME AUTORADIOGRAPHY

Joyce W. L. Ang[1,2], Arthur Bongrand[3,4], Samuel Duval[3], Jérôme Donnard[3], Risto Koivula[1], Marja Siitari-Kauppi[1], Gareth T. W. Law[1]

[1] Radiochemistry Unit, Department of Chemistry, The University of Helsinki, Helsinki 00014, Finland
[2] Singapore Nuclear Safety and Research Initiative, National University of Singapore, 138602, Singapore
[3] AI4R, 2 rue Alfred Kastler, 44307, Nantes, France
[4] IMT Atlantique, Nantes Université, CNRS, SUBATECH, F-44000 Nantes, France

NUCLEAR SCIENCE AND TECHNOLOGY SYMPOSIUM (SYP)

OUTLINE OF PRESENTATION

1. What are ‘hot’ particles?
2. Applications of BeaQuant onto ‘hot’ particles
3. Sample Preparation
4. Techniques Used for Each Consideration

'HOT' PARTICLES

- Radioactive
- Microns size range
- Sources:
  - Illicit activities
  - Nuclear accidents
  - Weapons
  - Mining sites
  - Nuclear waste disposal

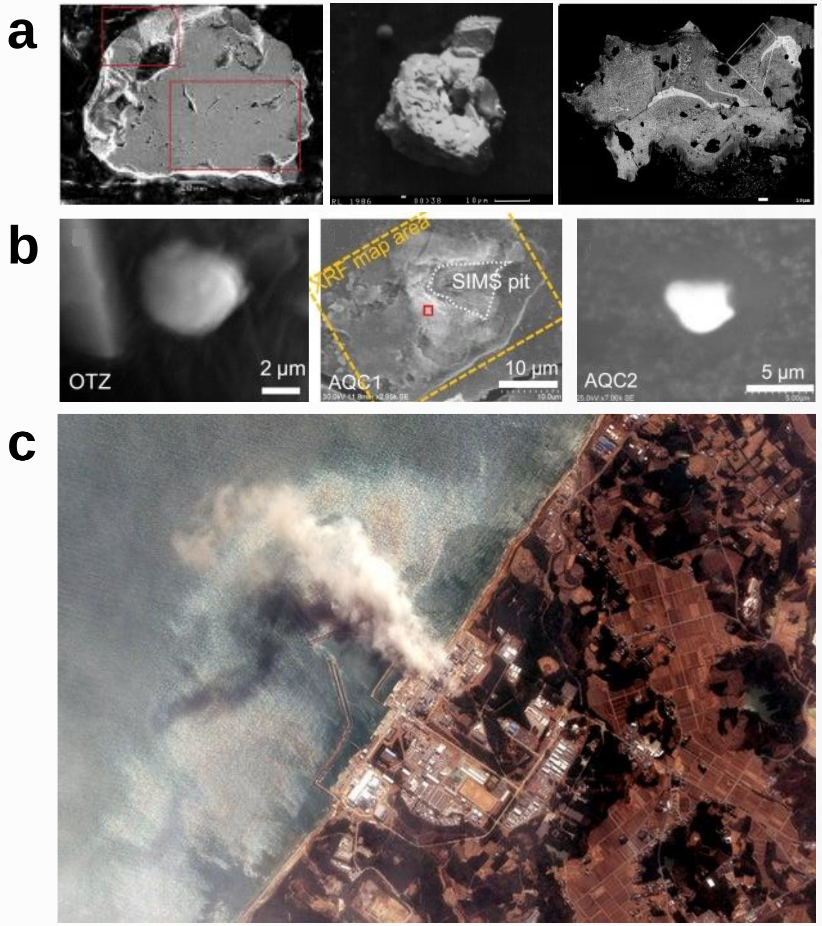

Fig 1. Hot particles from (a) Chernobyl, (b) Fukushima Daiichi accident. (c) Fukushima Daiichi nuclear power plant during the nuclear meltdown.

Image (a) adapted from DOI: 10.1016/j.jnucmat.2018.09.003; Image (b) adapted from DOI: 10.1016/j.scitotenv.2020.140539; Image (c) obtained from: https://www.scientificamerican.com/article/radioactive-glass-beads-may-tell-the-terrible-tale-of-how-the-fukushima-meltdown-unfolded/

'Hot' Particles | BeaQuant | Sample Prep | Detection

STUDYING ‘HOT’ PARTICLES

- Why study them
  - Fate of the particles
  - Remediation efforts

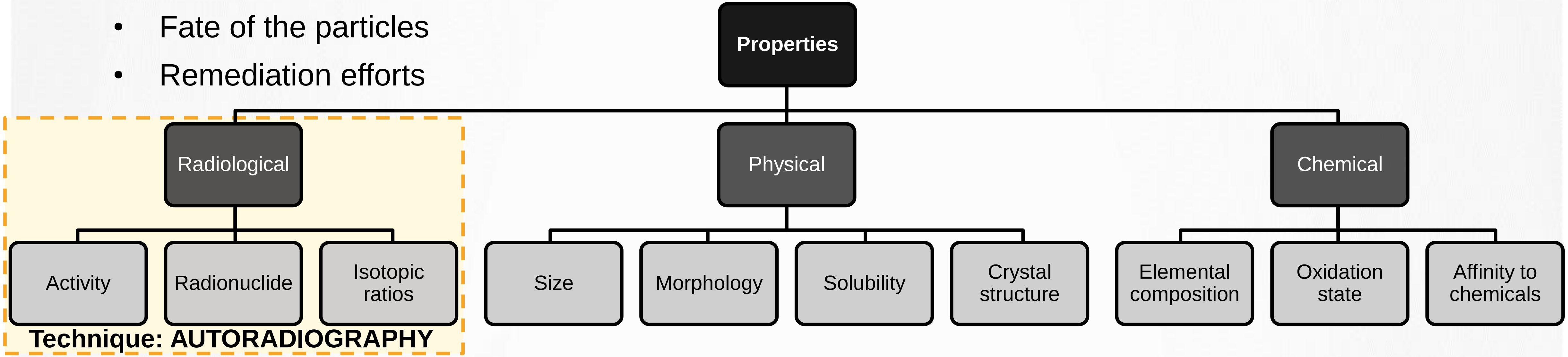

Fig 2. Classification of different properties that could be studied.

AUTORADIOGRAPHY OF 'HOT' PARTICLES

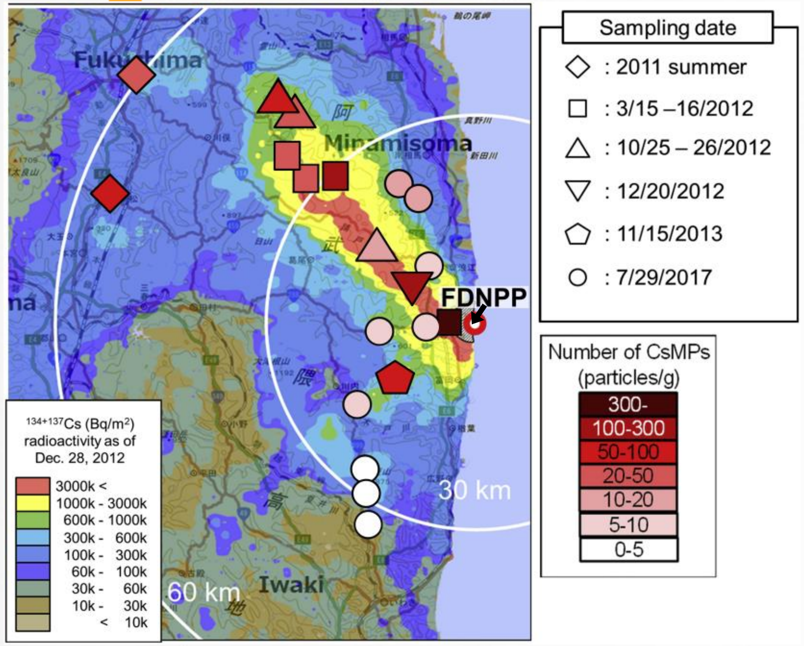

Fig 3. Map of $^{134+137}$Cs radioactivity distribution and number of CsMPs in sample sites in Japan.

Map adapted from: DOI 10.1016/j.chemosphere.2019.125019

Sieving
↓
Autoradiography
↓
Add droplets of water to 'hot' spots
↓
Take up the water with suspensions
↓
Carbon tape on 'hot' spots
↓
Cut carbon tape into smaller pieces with a blade
↓
Autoradiography and SEM

If suspension contains significant amount of soil

Fig 5. Particle isolation process.

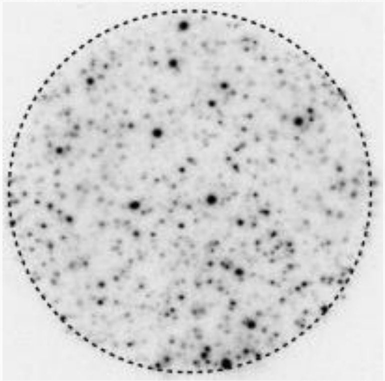

Fig 4. Autoradiograph of hot particles in filters

Image adapted from: DOI 10.1038/srep02554

'Hot' Particles → BeaQuant → Sample Prep → Detection

INTRODUCING BEAQUANT

Gas: Ne(90%)CO_2(10%)
Pressure: 1.1 bar

Fig 6. Picture of BeaQuant™.
Image obtained from AI4R.

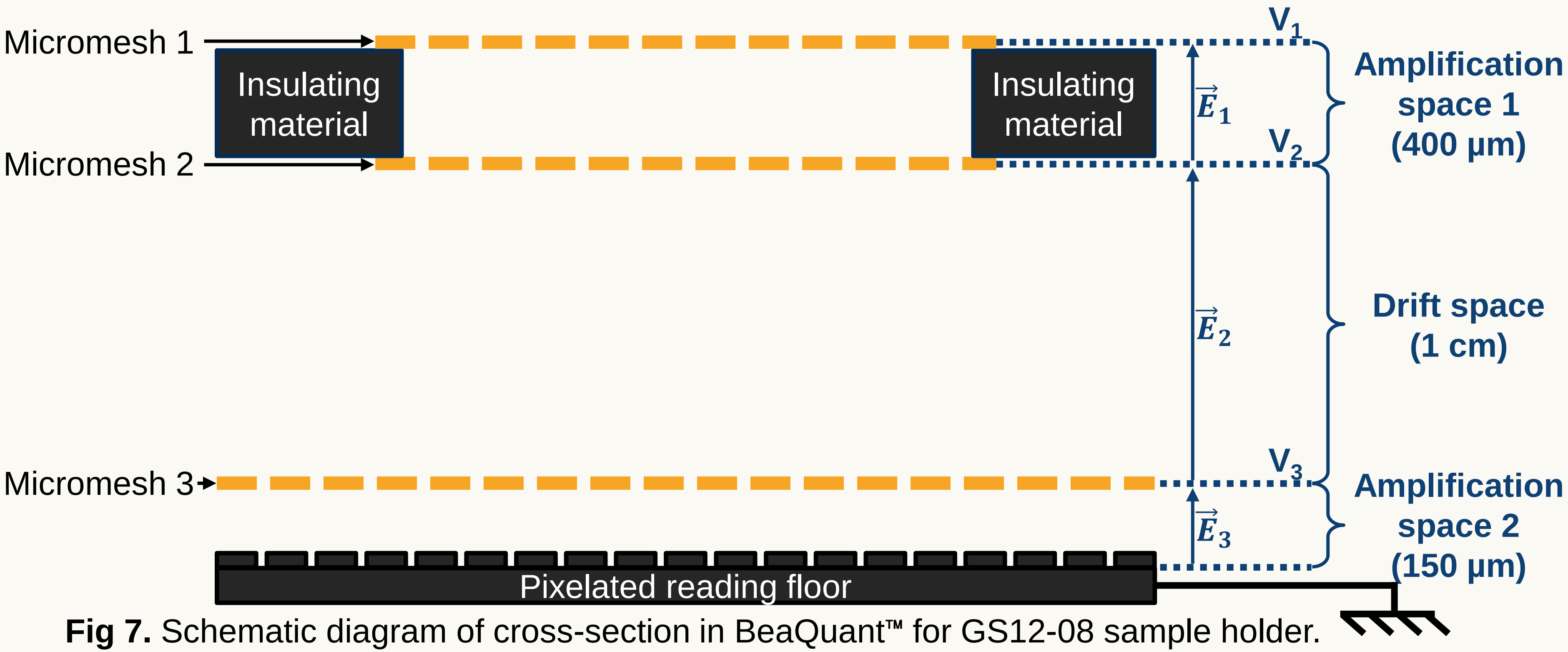

Fig 7. Schematic diagram of cross-section in BeaQuant™ for GS12-08 sample holder.

'Hot' Particles | **BeaQuant** | Sample Prep | Detection

INTRODUCING BEAQUANT

Fig 6. Picture of BeaQuant™.

Image obtained from AI4R.

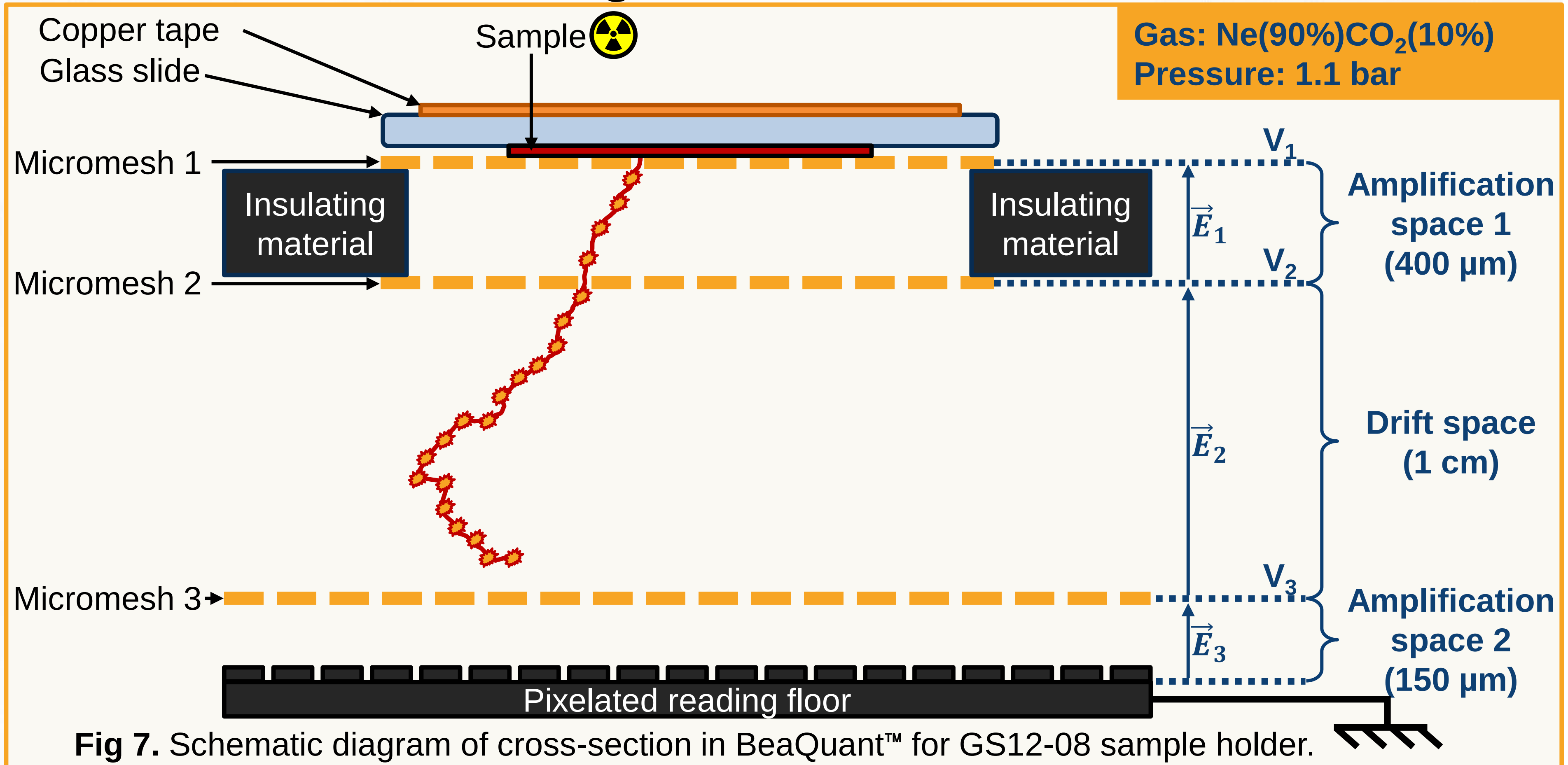

Fig 7. Schematic diagram of cross-section in BeaQuant™ for GS12-08 sample holder.

'Hot' Particles | BeaQuant | Sample Prep | Detection

INTRODUCING BEAQUANT

Fig 6. Picture of BeaQuant™.

Image obtained from AI4R.

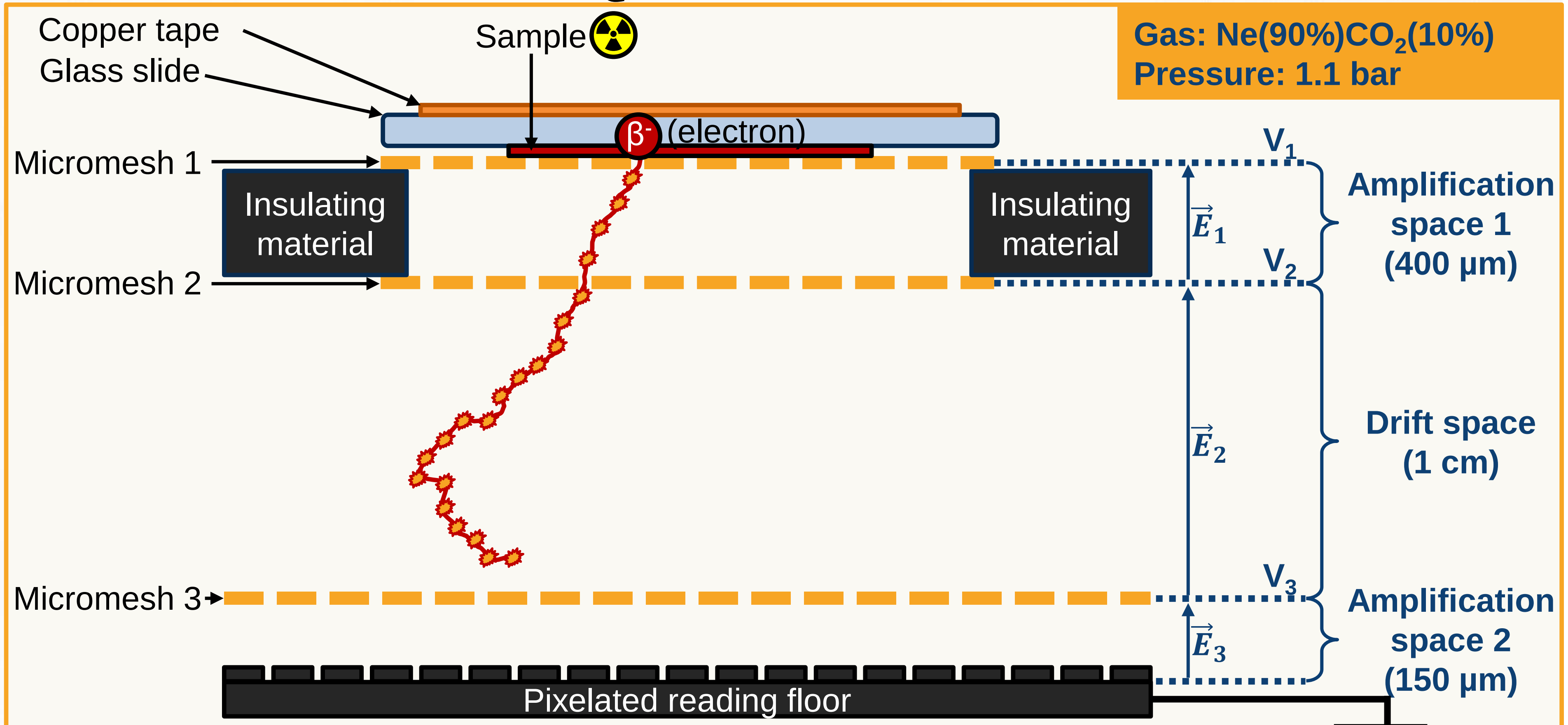

Fig 7. Schematic diagram of cross-section in BeaQuant™ for GS12-08 sample holder.

INTRODUCING BEAQUANT

Fig 6. Picture of BeaQuant™.

Image obtained from AI4R.

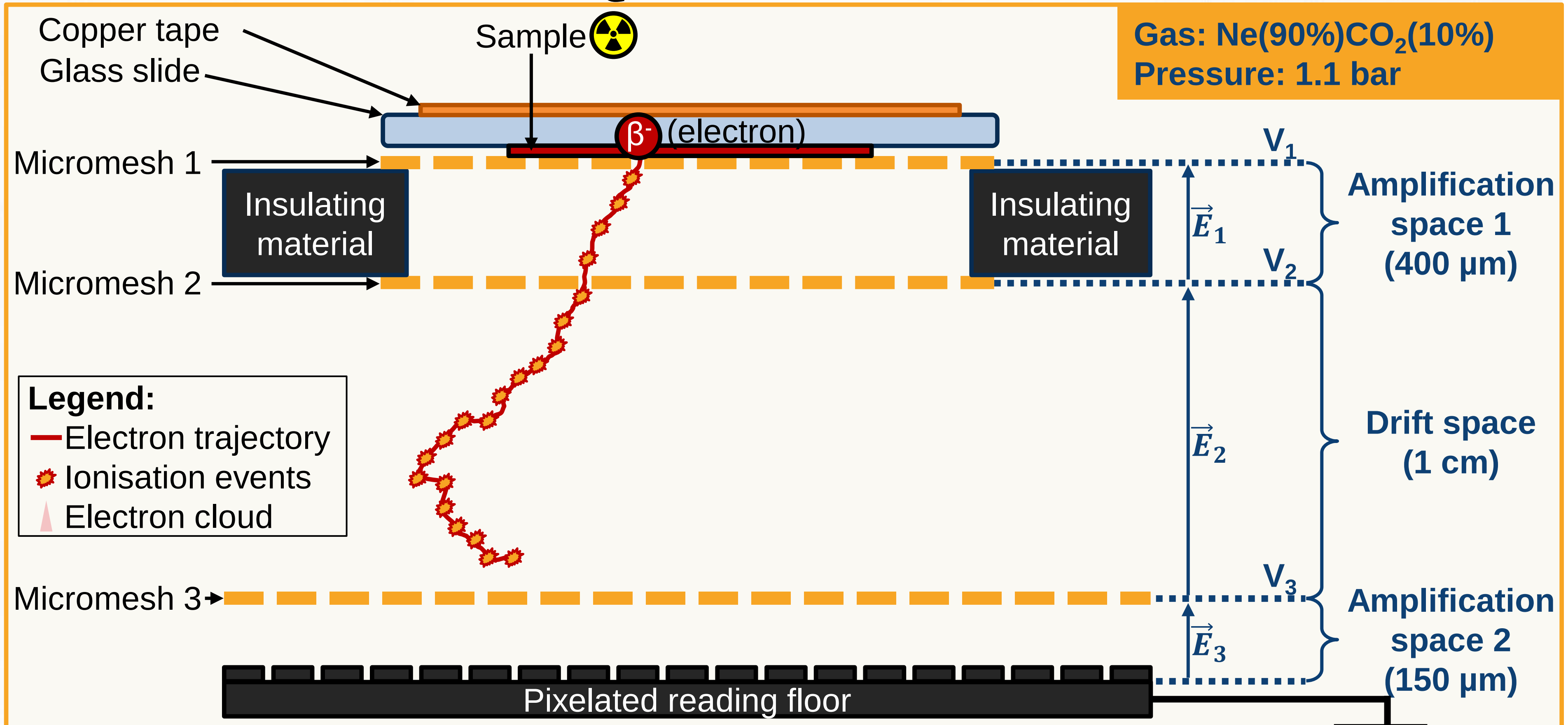

Fig 7. Schematic diagram of cross-section in BeaQuant™ for GS12-08 sample holder.

INTRODUCING BEAQUANT

Fig 6. Picture of BeaQuant™.

Image obtained from AI4R.

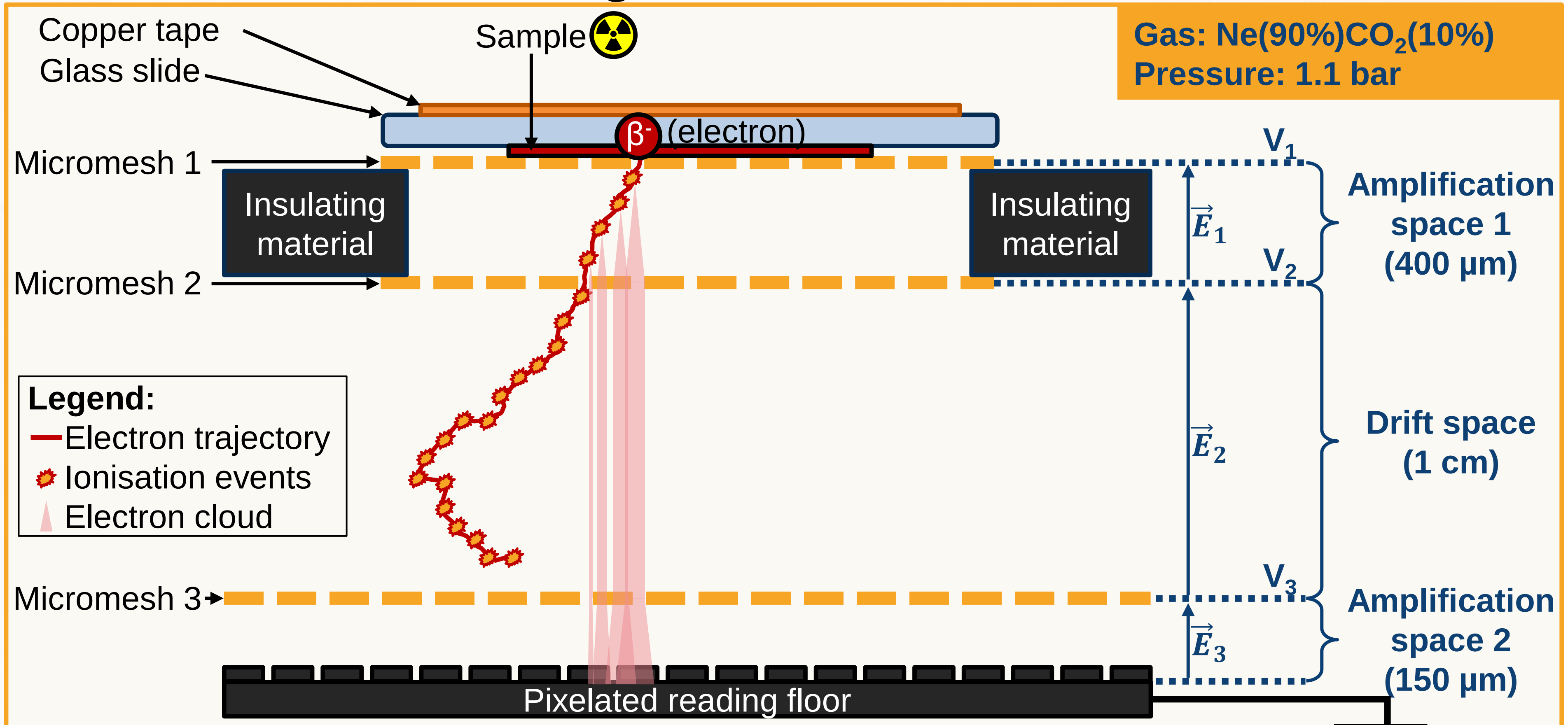

Fig 7. Schematic diagram of cross-section in BeaQuant™ for GS12-08 sample holder.

'Hot' Particles | **BeaQuant** | Sample Prep | Detection

INTRODUCING BEAQUANT

Fig 6. Picture of BeaQuant™.

Image obtained from AI4R.

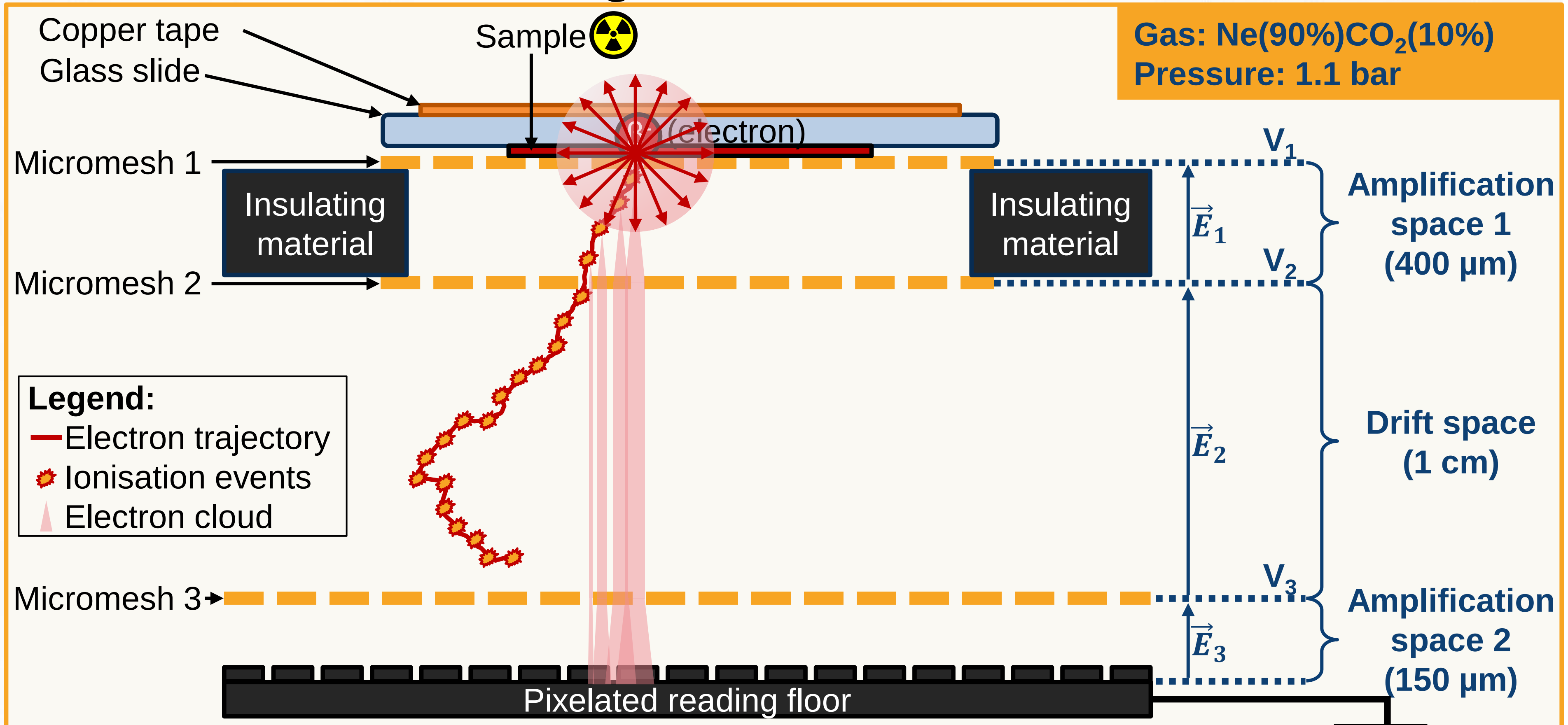

Fig 7. Schematic diagram of cross-section in BeaQuant™ for GS12-08 sample holder.

'Hot' Particles | BeaQuant | Sample Prep | Detection

INTRODUCING BEAQUANT

Fig 6. Picture of BeaQuant™.
Image obtained from AI4R.

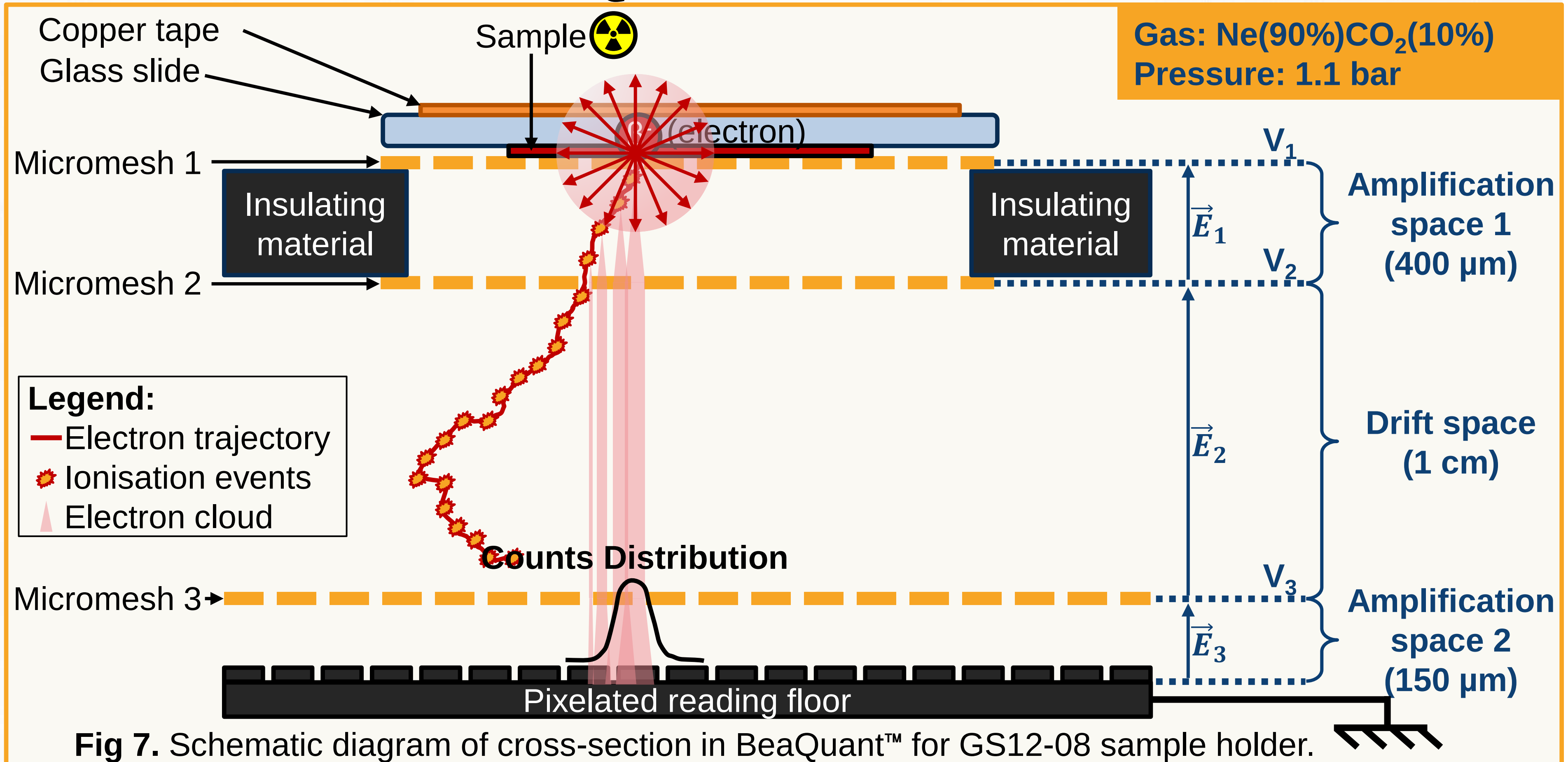

Fig 7. Schematic diagram of cross-section in BeaQuant™ for GS12-08 sample holder.

'Hot' Particles | **BeaQuant** | Sample Prep | Detection

ADVANTAGES OF BEAQUANT

BeaQuant	Phosphor Screen Autoradiography
Real-time→ Faster accident response	Not real-time
Possibility of performing spectrometry	Possible (but tedious) for differentiating alpha vs beta

Direct measurement

Fig 8. Sample loaded onto micromesh.

2-step approach

Exposure → Scanning

Fig 9. Series of steps from exposing sample on imaging plate to loading imaging plate into scanner.

'Hot' Particles → BeaQuant → Sample Prep → Detection

ADVANTAGES OF BEAQUANT

BeaQuant	Phosphor Screen Autoradiography
Real-time→ Faster accident response	Not real-time
Possibility of performing spectrometry	Possible (but tedious) for differentiating alpha vs beta

Fig 10. Deconvolution of H-3 and C-14.
Images obtained from AI4R.

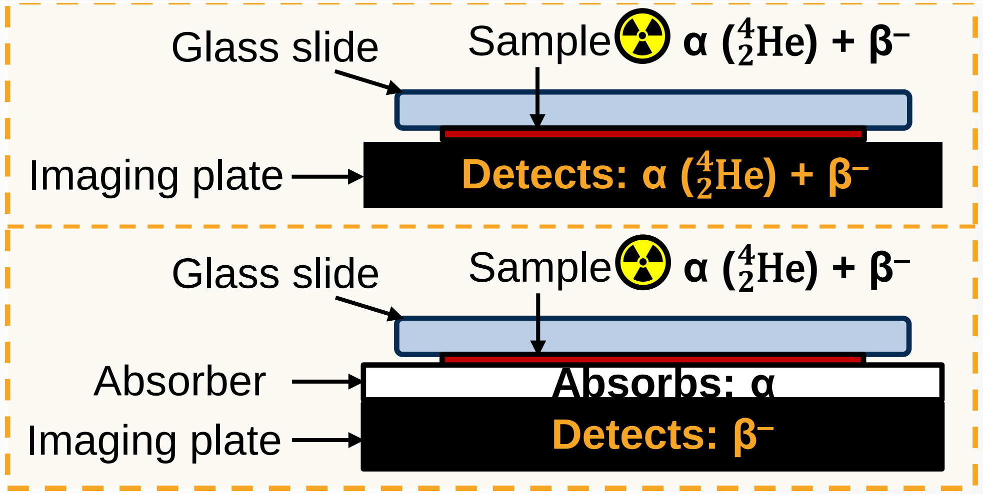

Fig 11. Separation of α from β using phosphor screen autoradiography.

‘Hot’ Particles | BeaQuant | Sample Prep | Detection

TOPICS OF CONSIDERATION

- Sample preparation
  - Methodology
  - Sample thickness
- Detection
  - Cs calibration
  - Deconvolution by energy spectra
  - Spatial resolution
  - Artefact contribution

+ GEANT4 A SIMULATION TOOLKIT

'Hot' Particles | BeaQuant | Sample Prep | Detection

TYPES OF SAMPLES

- Cesium: Cs-134, Cs-137
- Form
  - Simple ‘massless’ samples
  - Particulate matrix
  - Sediments

‘Hot’ Particles | BeaQuant | Sample Prep | Detection

PREPARING SIMPLE ‘MASSLESS’ SAMPLES

- ‘Massless’ samples
  - Deposition using evaporation technique
- Varying activity concentration
  - Serial dilution
- Wrapped with 3-microns mylar film

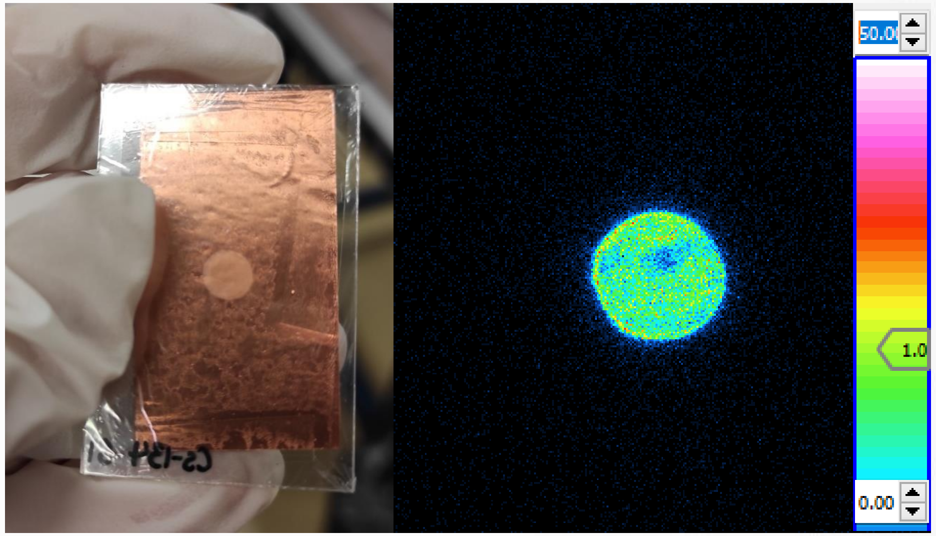

Fig 12. Example of a thin ‘massless’ sample and their autoradiograph from BeaQuant.

‘Hot’ Particles | BeaQuant | Sample Prep | Detection

CS CALIBRATION

Table 1. Intrinsic efficiency and minimum detectable activity (MDA) per unit area for Cs-137 and Cs-134.

Radionuclide	Intrinsic Efficiency (%)	MDA per Unit Area (mBq/mm^2)
Cs-137	16.4 ± 1.3	1.02
Cs-134	22.7 ± 0.6	0.947

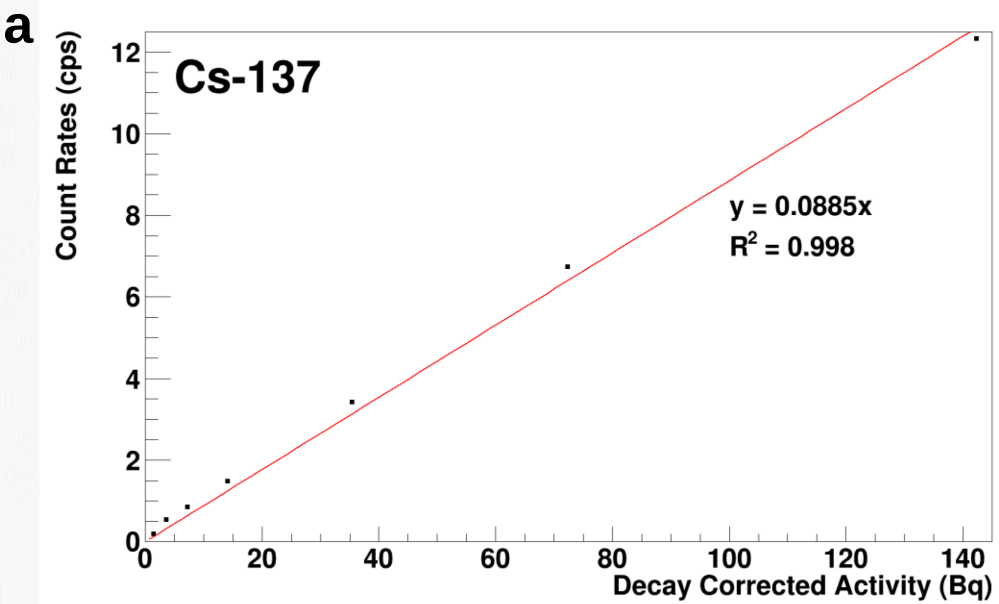

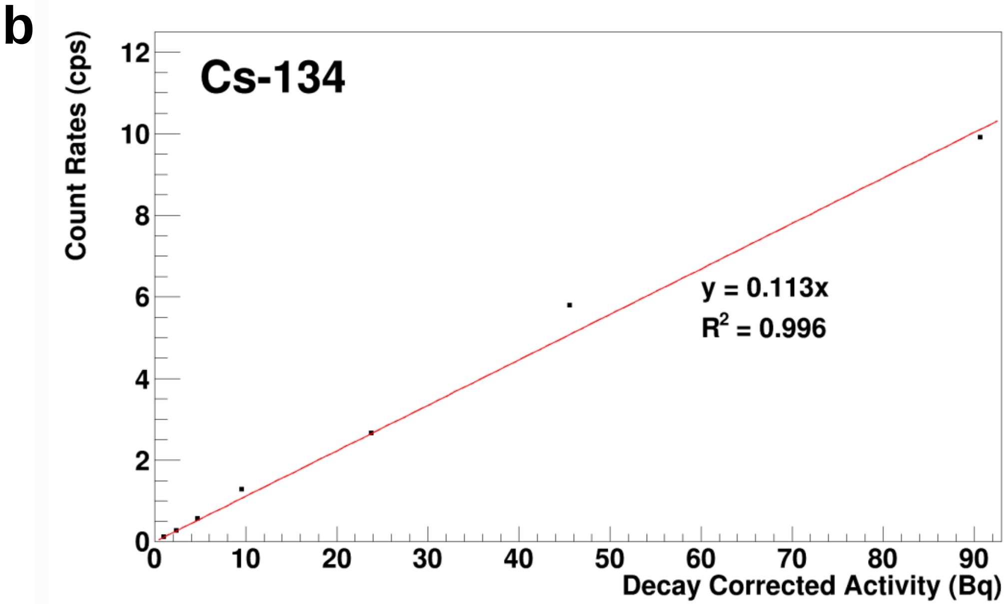

Fig 13. Activity sample calibration curve for (a) Cs-137 and (b) Cs-134 'massless' samples. Error bars (calculated from counting statistics) are too small to be seen in these graphs.

'Hot' Particles | BeaQuant | Sample Prep | Detection

CS DECONVOLUTION

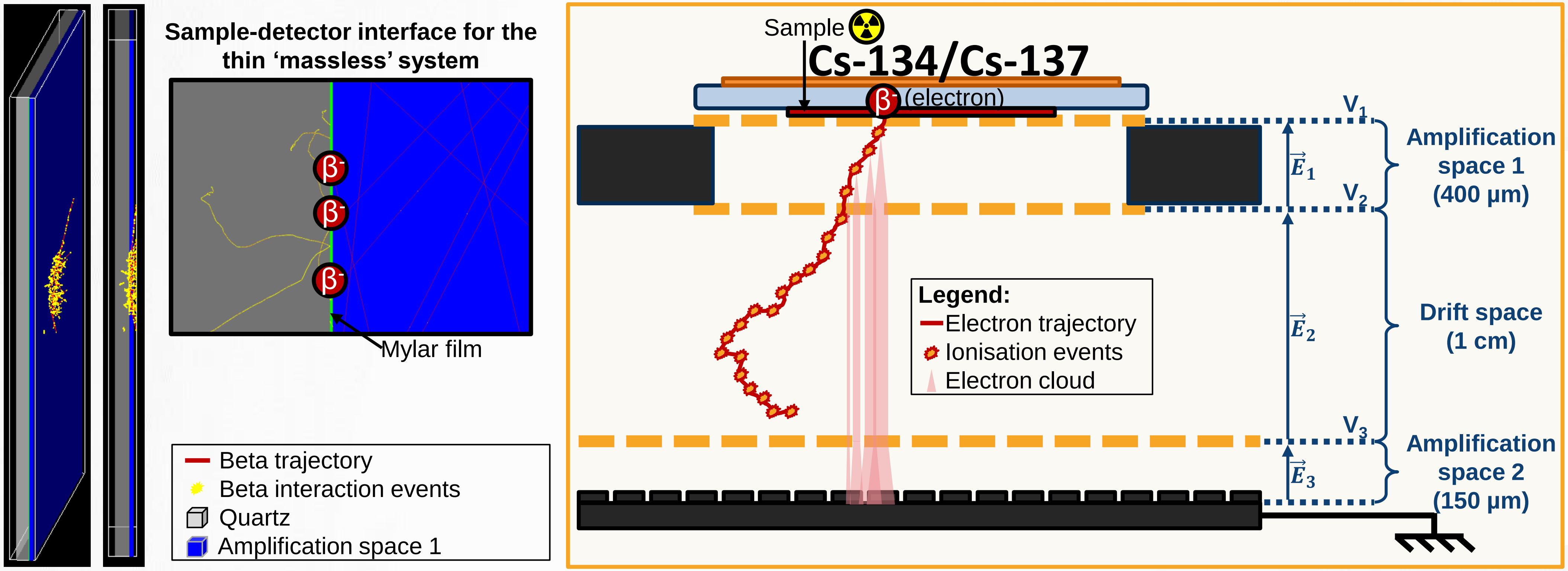

Fig 14. GEANT4 simulation of the emitted electrons from the Cs-134 and Cs-137 decay for the massless samples.

'Hot' Particles | BeaQuant | Sample Prep | Detection

CS DECONVOLUTION

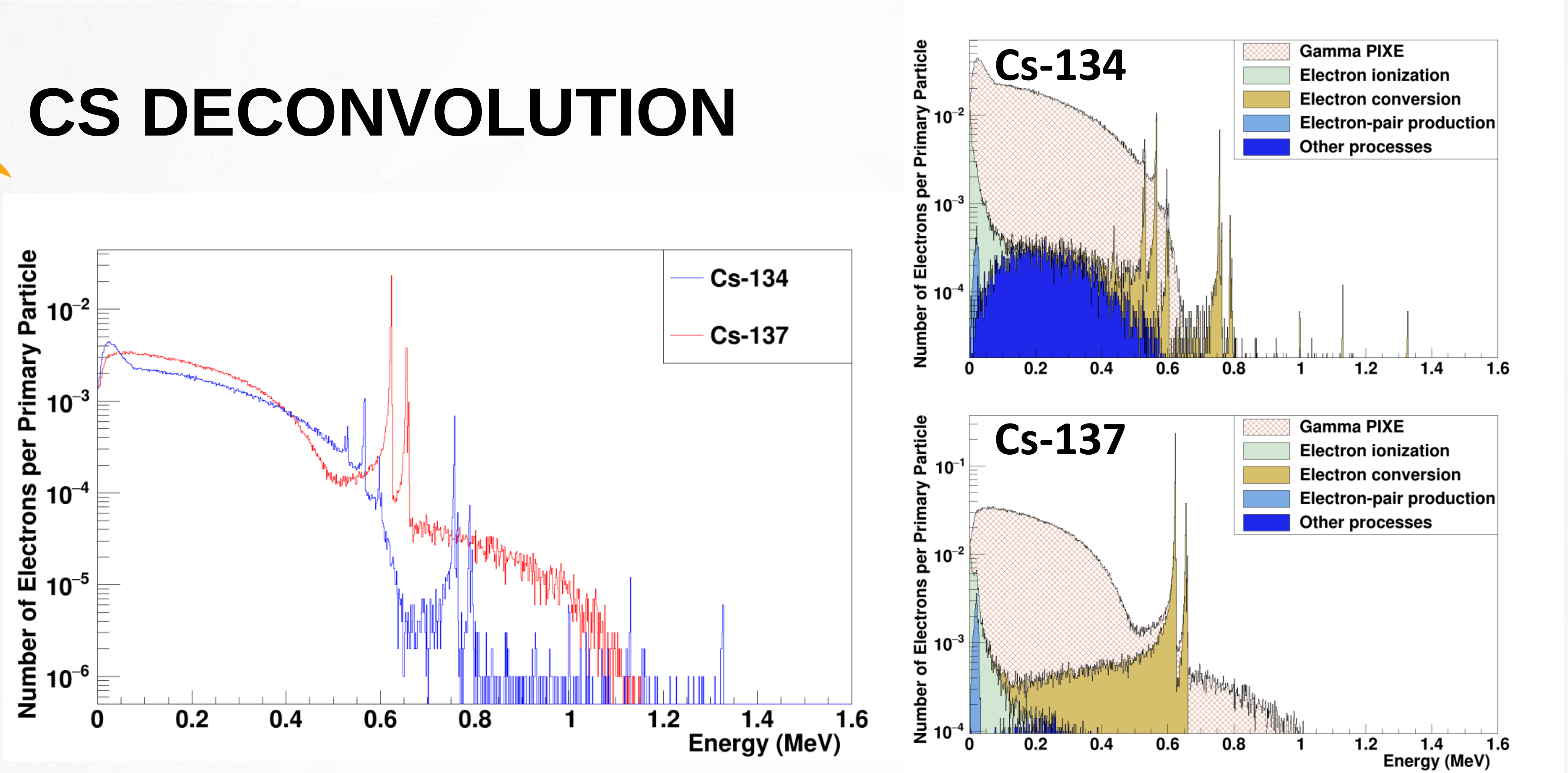

Fig 14. GEANT4 simulation of the emitted electrons from the Cs-134 and Cs-137 decay for the massless samples.

‘Hot’ Particles | BeaQuant | Sample Prep | Detection

CS DECONVOLUTION

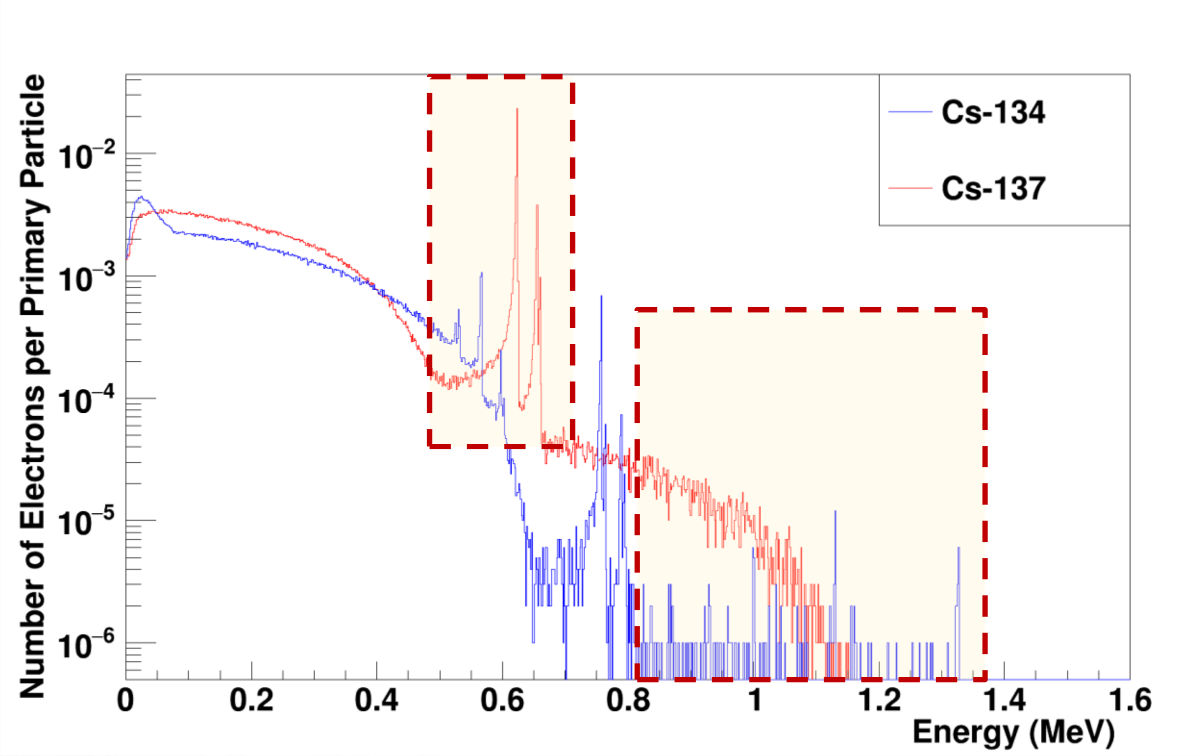

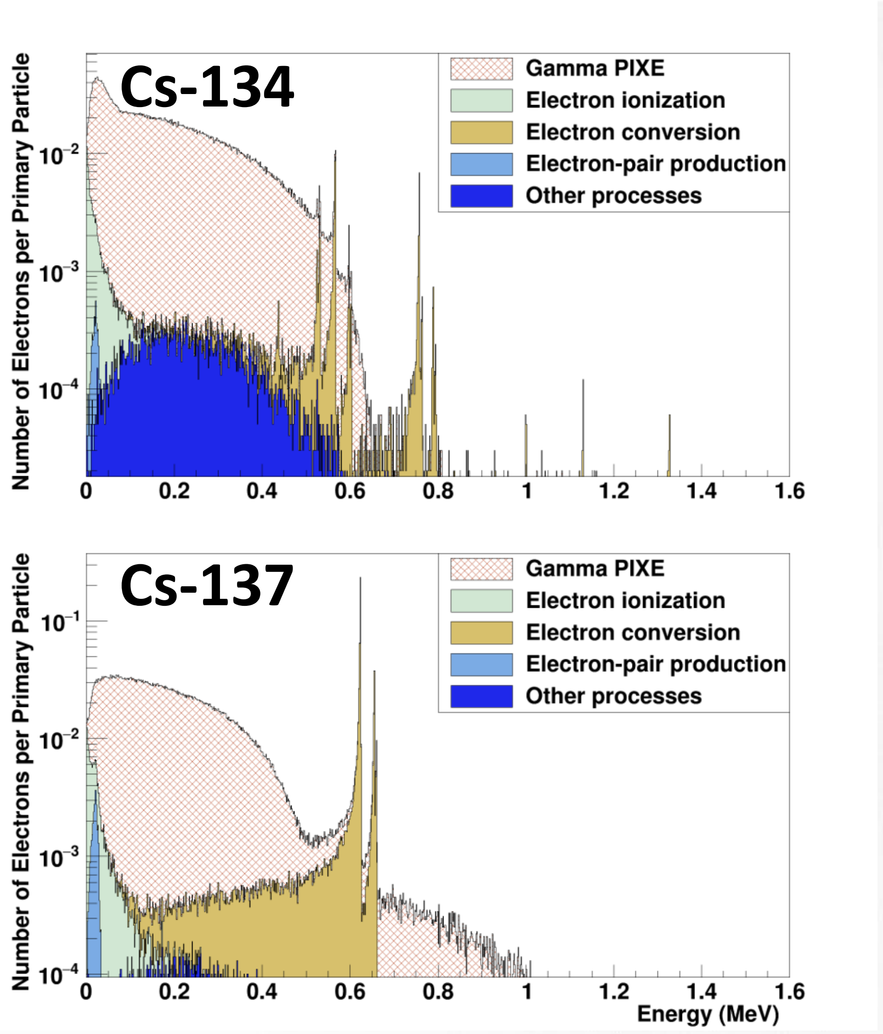

Fig 14. GEANT4 simulation of the emitted electrons from the Cs-134 and Cs-137 decay for the massless samples.

'Hot' Particles | BeaQuant | Sample Prep | Detection

CS DECONVOLUTION

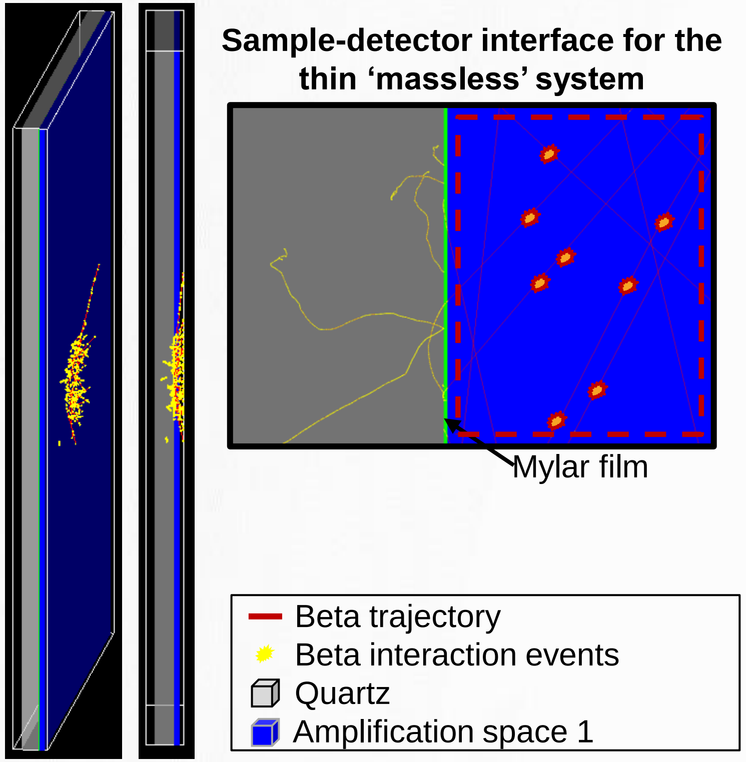

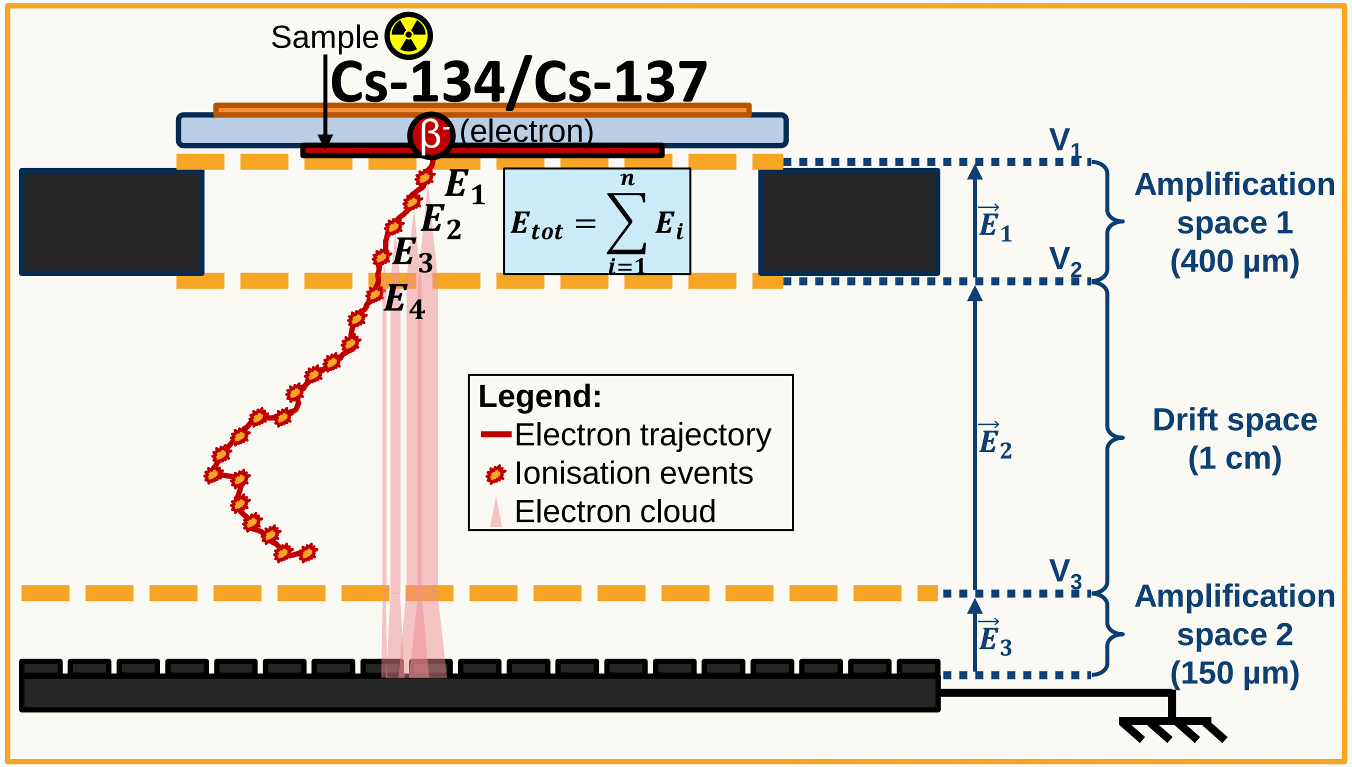

'Hot' Particles | BeaQuant | Sample Prep | **Detection**

CS DECONVOLUTION

a

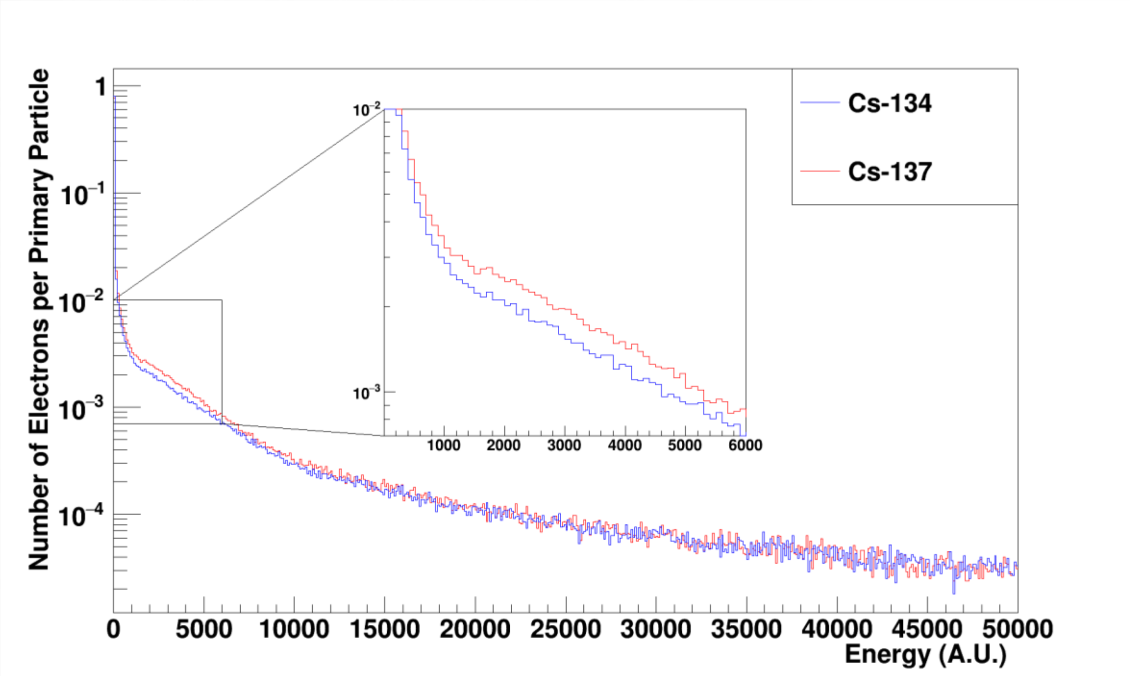

b

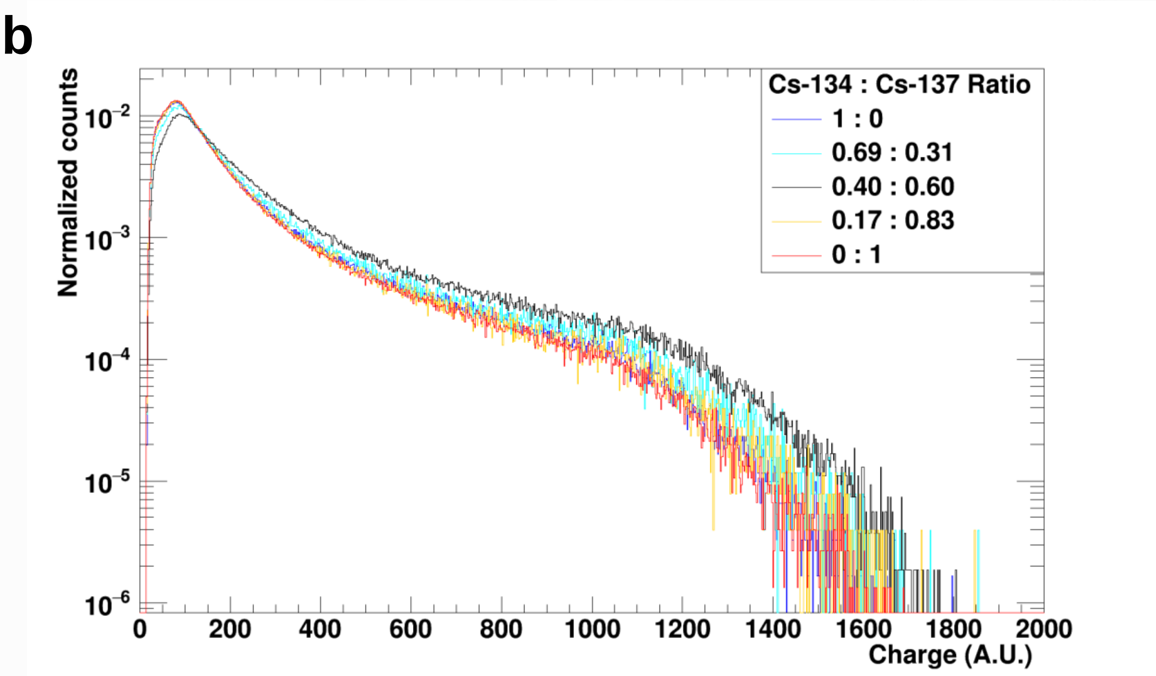

Fig 15. Energy deposited by electrons emitted from Cs-134 and Cs-137 radiation decay from (a) GEANT4 simulations and (b) actual BeaQuant™ results.

'Hot' Particles | BeaQuant | Sample Prep | Detection

CS SORPTION ON PARTICLES

- Minerals were coated with Cs-134 or Cs-137
  - CsCl solution, pH 7
  - Copper hexacyanoferrate (Cu HCF)
  - Quartz
  - Illite
  - Weathered biotite

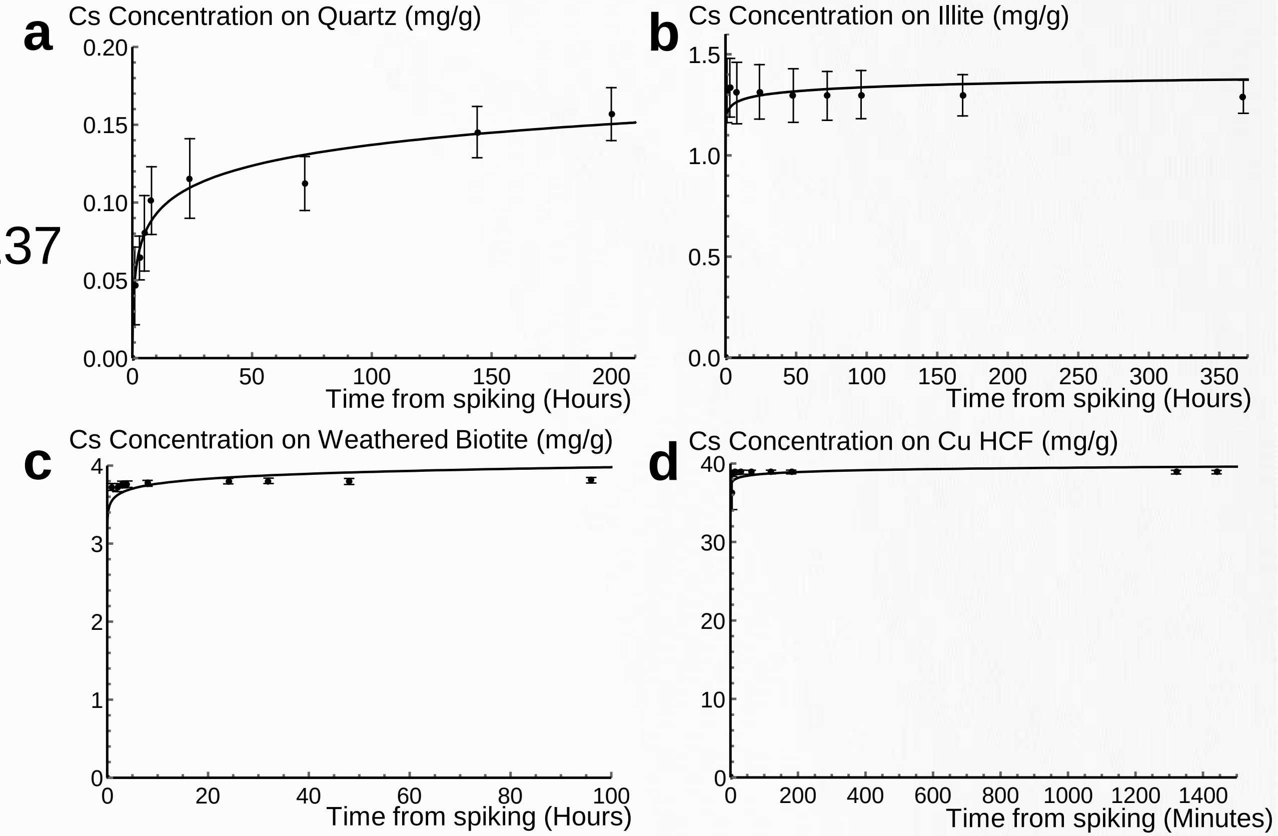

Fig 16. Adsorption of caesium on (a) quartz, (b) illite, (c) weathered biotite, and (d) Cu HCF.

'Hot' Particles | BeaQuant | Sample Prep | Detection

PREPARING RESIN EMBEDDED SAMPLES

- Resin embedded with epoxy resin (Araldite® M and Ren™ HY956)
- Sawed to thin slices, adhered onto glass slides
- Polished (80, 500, 1200 and 2000 grit size)

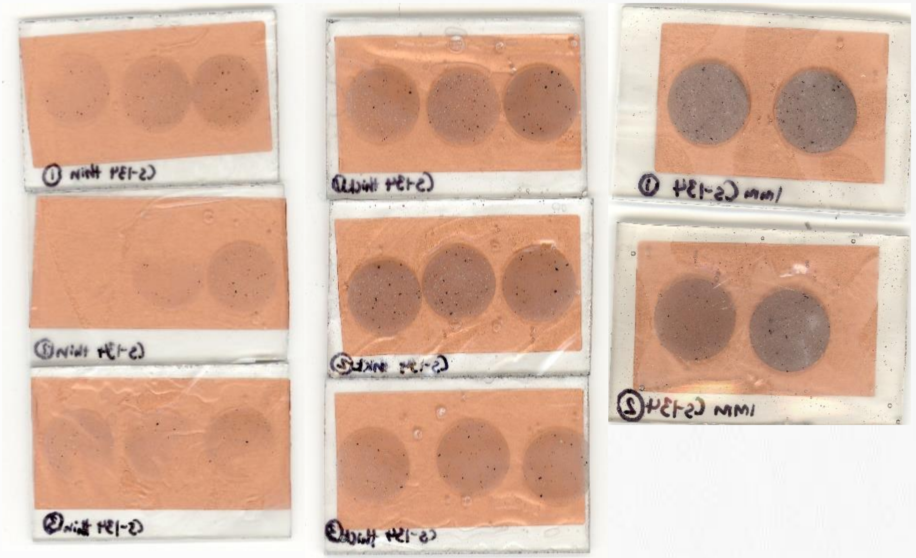

Fig 17. Example images of resin embedded samples.

'Hot' Particles | BeaQuant | Sample Prep | Detection

SAMPLE THICKNESS

- Study how sample thickness affects signal
- GEANT4 simulation

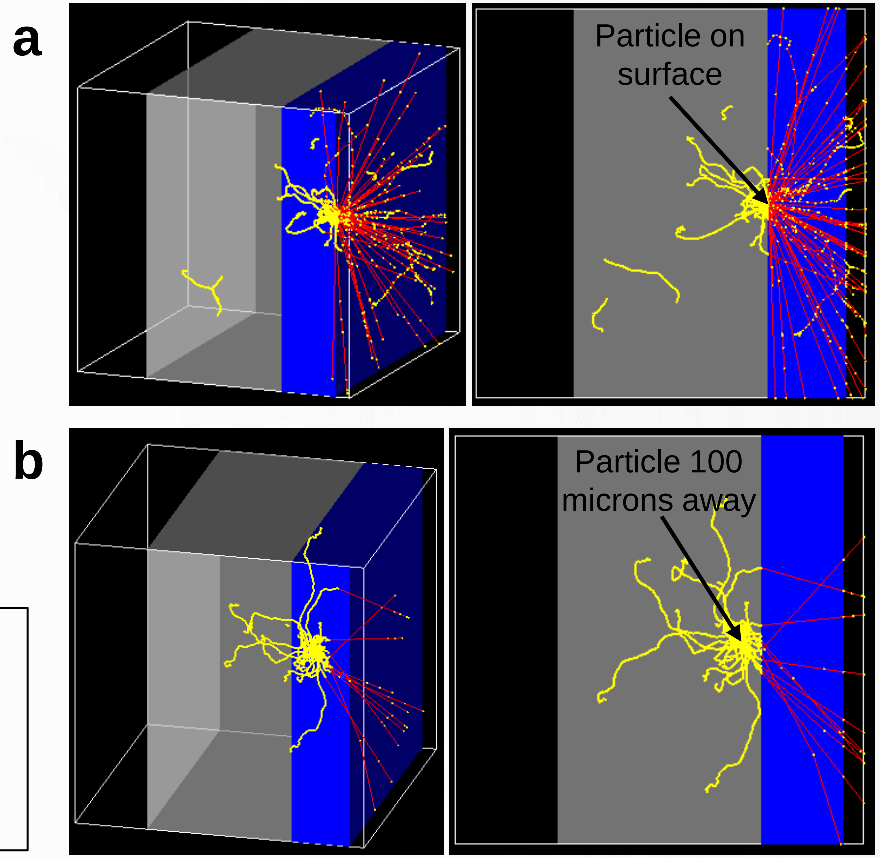

Legend:
Beta trajectory
Beta interaction events
Quartz
Amplification gap

Fig 18. GEANT4 simulation of 100 decay events for a Cs-134 particle which is (a) on surface of sample and (b) 100 microns depth from sample surface.

SAMPLE THICKNESS

- Study how sample thickness affects signal
- GEANT4 simulation

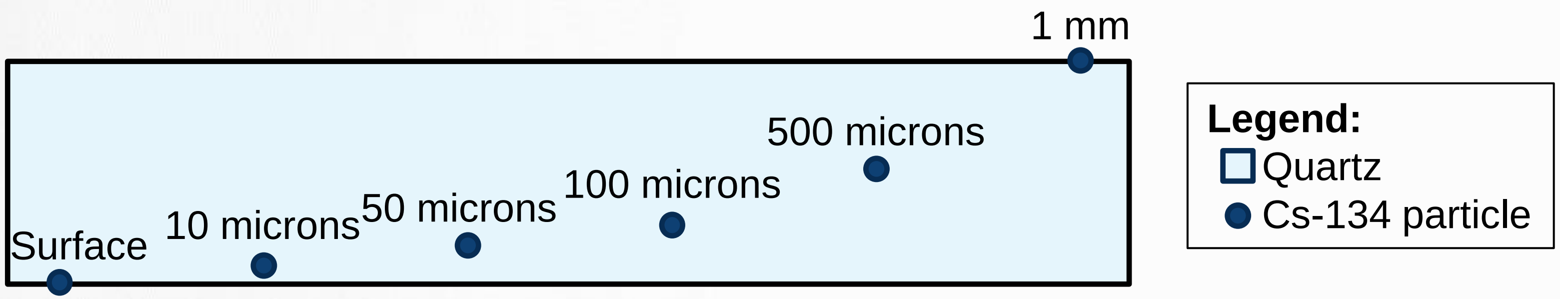

Fig 19. GEANT4 simulation scenario for different sample particle depth.

SAMPLE THICKNESS

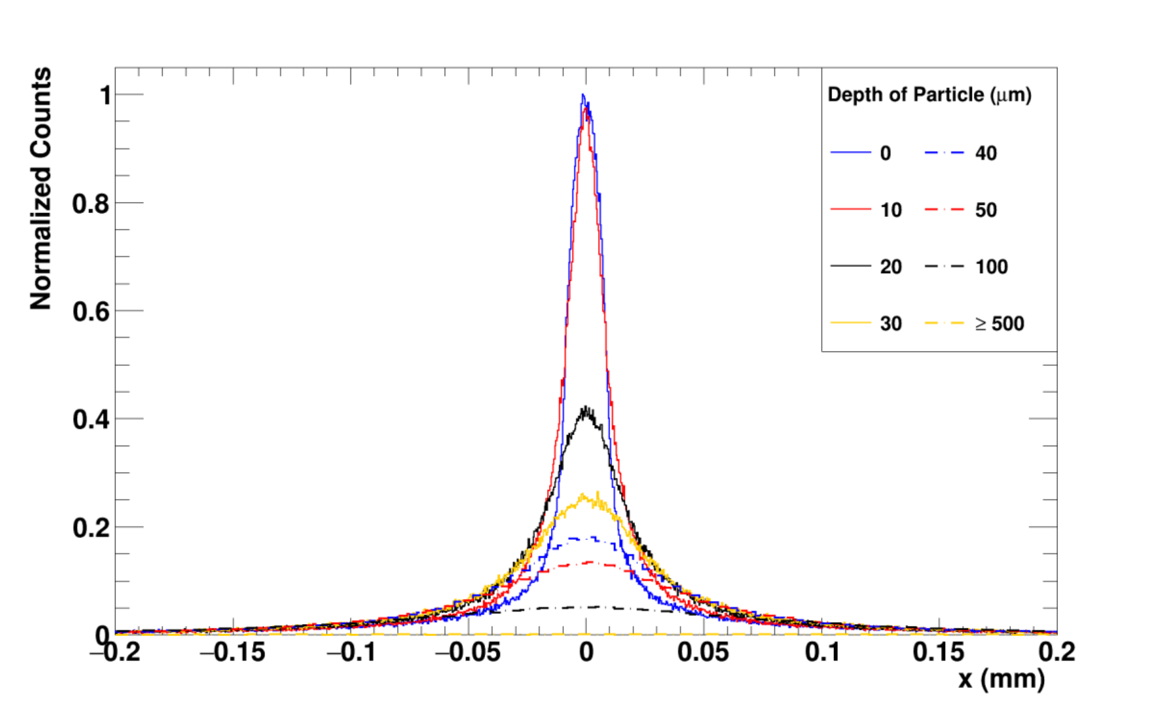

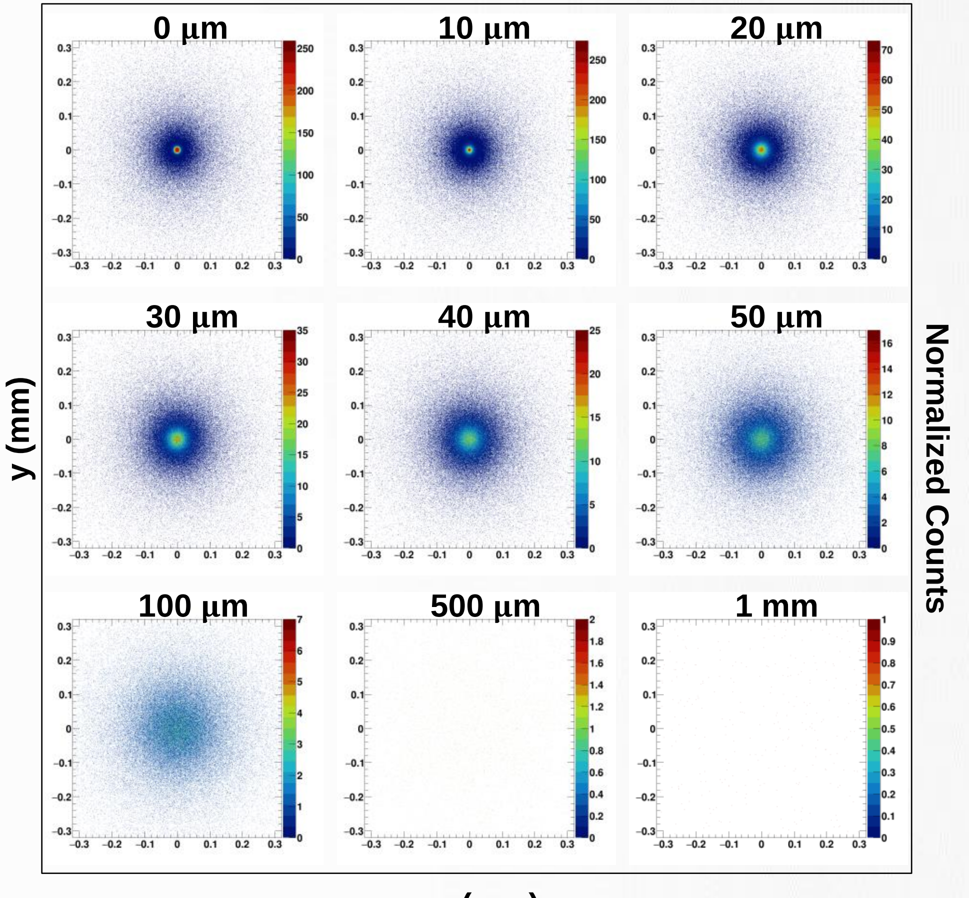

Fig 20. GEANT4 simulation (1 decay million events) results for a Cs-134 particle with varying depths from sample surface.

‘Hot’ Particles | BeaQuant | Sample Prep | Detection

SAMPLE THICKNESS

- Study how sample thickness affects signal
- GEANT4 simulation
- Samples of different thicknesses
  - 10s of microns, 100s of microns, 1 mm

Table 2. Full-width at half maximum and background baseline for different sample thicknesses.

Sample Thickness (µm)	Average FWHM (mm)	Baseline (Normalized Counts)
70 ± 40	0.6 ± 0.3	0.05–0.13
680 ± 30	0.9 ± 0.6	0.07–0.18
1000 ± 200	0.4 ± 0.1	0.12–0.21

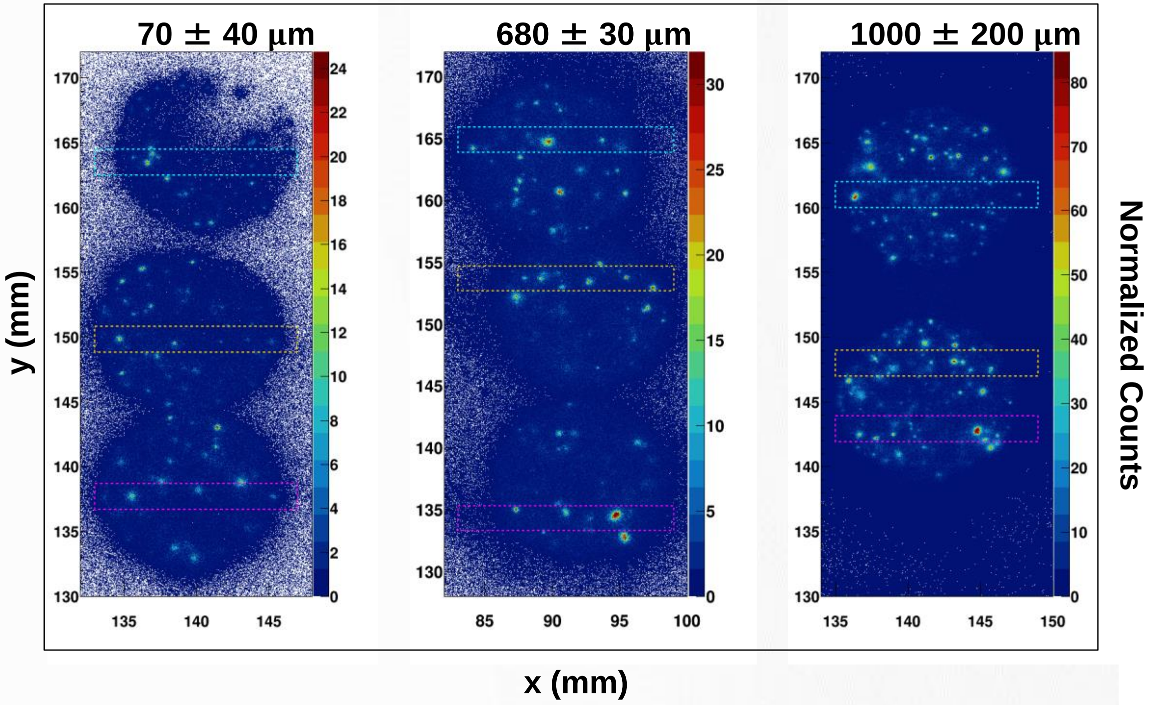

Fig 21. Comparison of autoradiograph from a thin sample and a thick sample.

‘Hot’ Particles | BeaQuant | Sample Prep | Detection

X-RAY CT – IDENTIFYING 4 PARTICLES

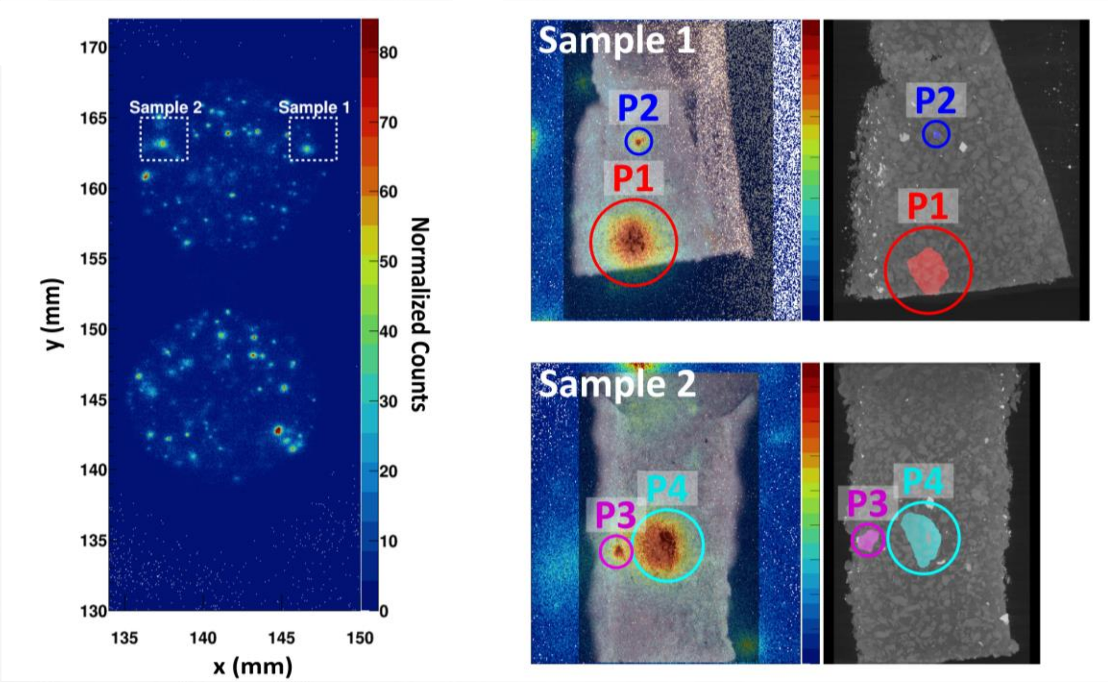

Fig 22. Autoradiograph, microscope, and X-ray CT images.

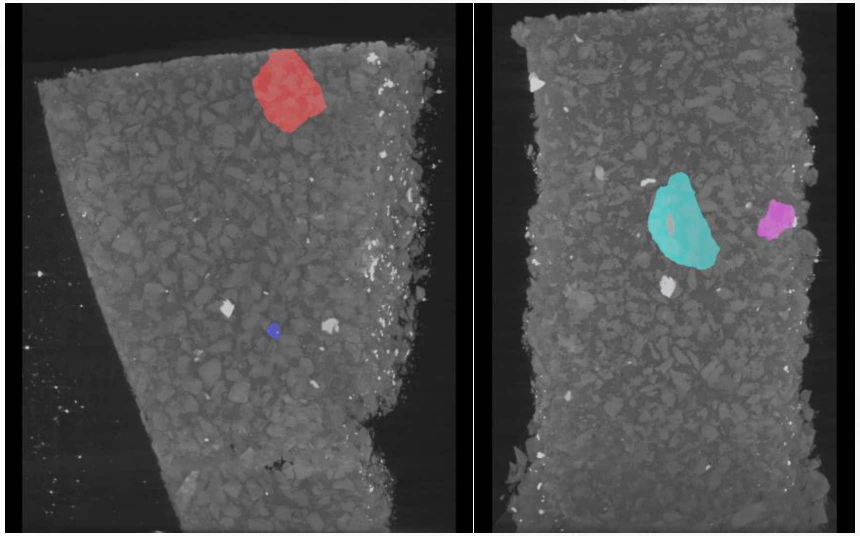

Table 3. Particle sizes and depth, obtained from X-ray CT.

Particle	Depth (µm)	Semi-axis A (µm)	Semi-axis B (µm)	Semi-axis C (µm)
P1	167	140	175	129
P2	28	29	33	28
P3	161	94	63	82
P4	240	126	212	210

‘Hot’ Particles | BeaQuant | Sample Prep | Detection

X-RAY CT – SIMULATION VS BEAQUANT

- Peak broadening
- Background contribution

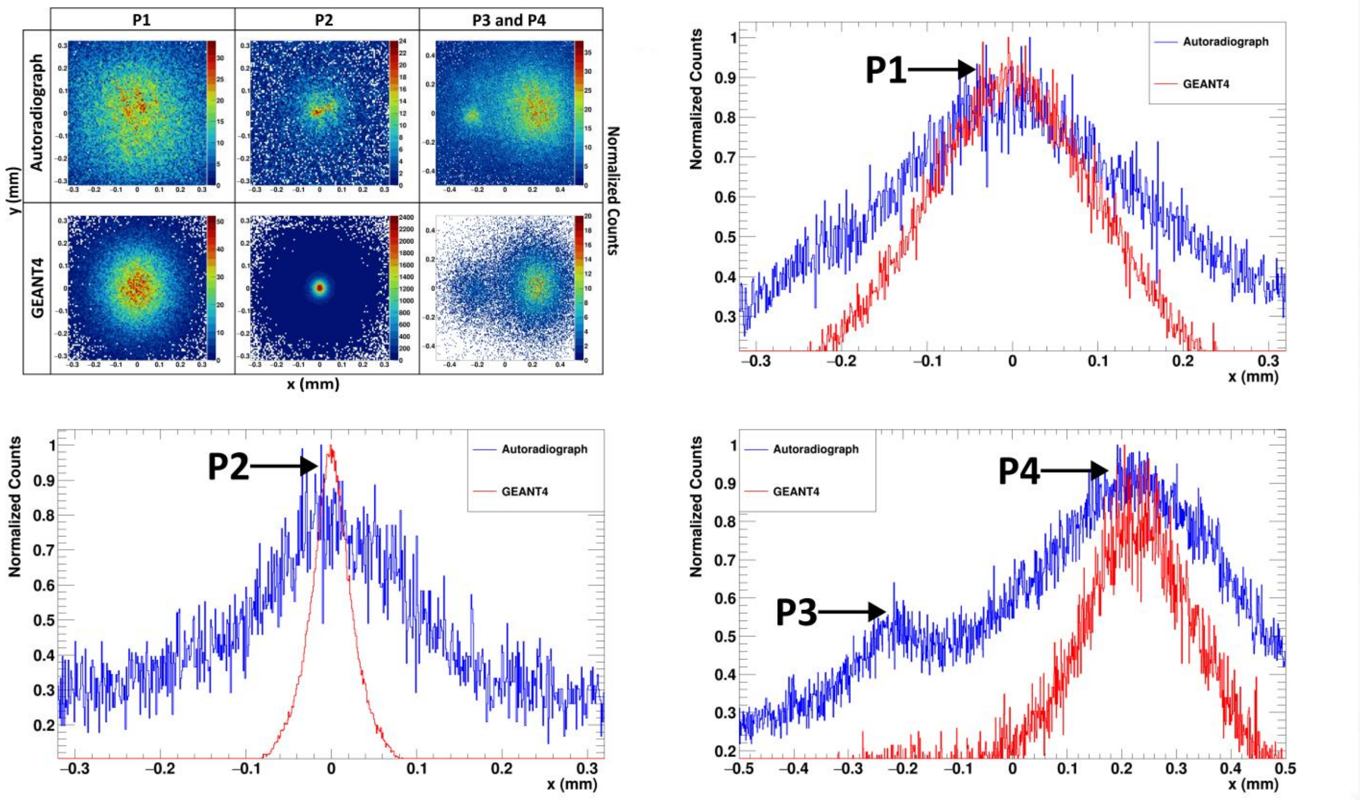

Fig 23. Comparison of GEANT4 simulation and BeaQuant™ autoradiographs for particles 1, 2, 3, and 4.

‘Hot’ Particles | BeaQuant | Sample Prep | Detection

SPATIAL RESOLUTION STUDIES

- Broadening of peaks due to detector
- Applied Gaussian blurring to GEANT4 simulation
  - CERN ROOT (version 6.19/02)
- Quantify spatial resolution

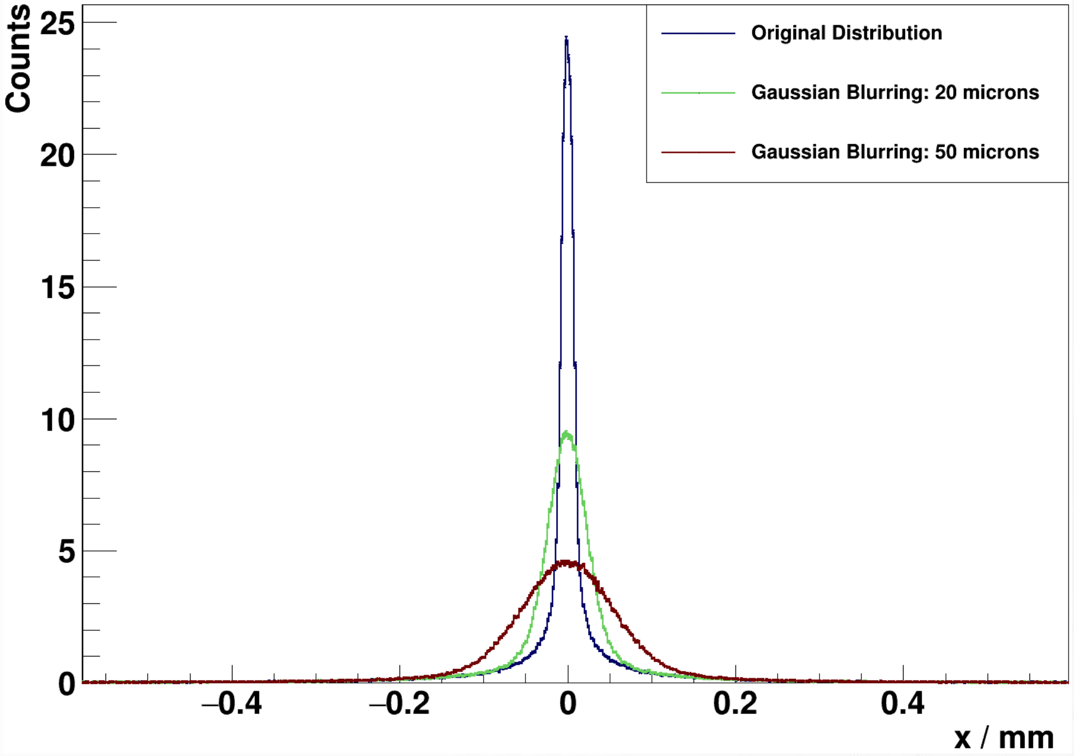

Fig 24. X distributions before and after gaussian blurring of 20 and 50 microns.

‘Hot’ Particles | BeaQuant | Sample Prep | **Detection**

ARTEFACT IDENTIFICATION

- Artefact contribution
  - Dust
  - Air pockets

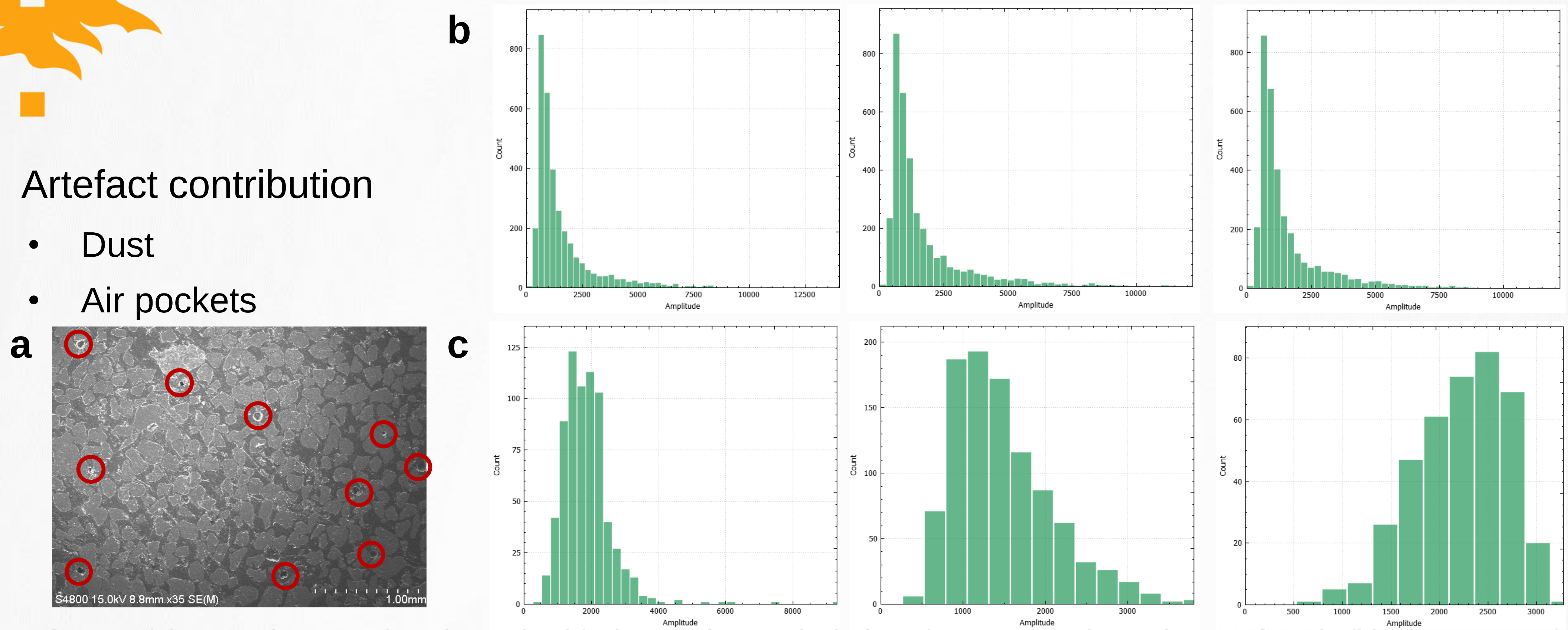

Fig 25. (a) SEM image of resin embedded sample. Red circles demarcate air pocket ‘defects’. (b) Counts against charge for 3 real Cs-134 hot particle signal, (c) Counts against charge for 3 artefacts.

FUTURE WORKS

- Library of data from hot particle and artefact contribution
- BeaQuant ability to identify particles in noisy background
- Improving the sample preparation

Table 4. Types of sediment and their Cs-134 activity concentration.

Type	Material	Size Fraction (μm)	Activity Concentration (MBq/g)
Particle	Copper HCF	< 25	55
Sediment	Weathered biotite	50 – 100	5
	Illite–smectite mixed layer (70/30)	50 – 100	0.5
	Quartz	50 – 100	0.5

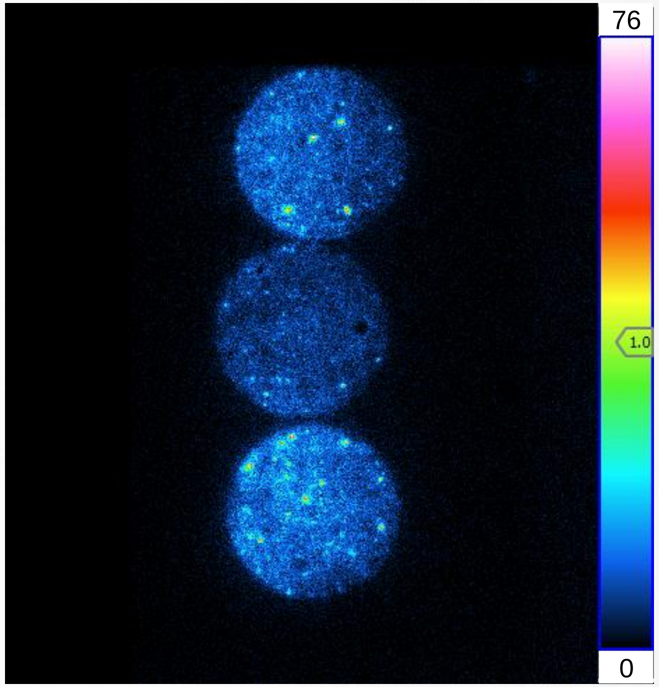

Fig 26. Autoradiograph of sediment sample (Cs particles in a lower radioactivity Cs sediments).

CONCLUSION

- BeaQuant and their relevance
- Sample preparation techniques
- Quantifying BeaQuant’s capabilities

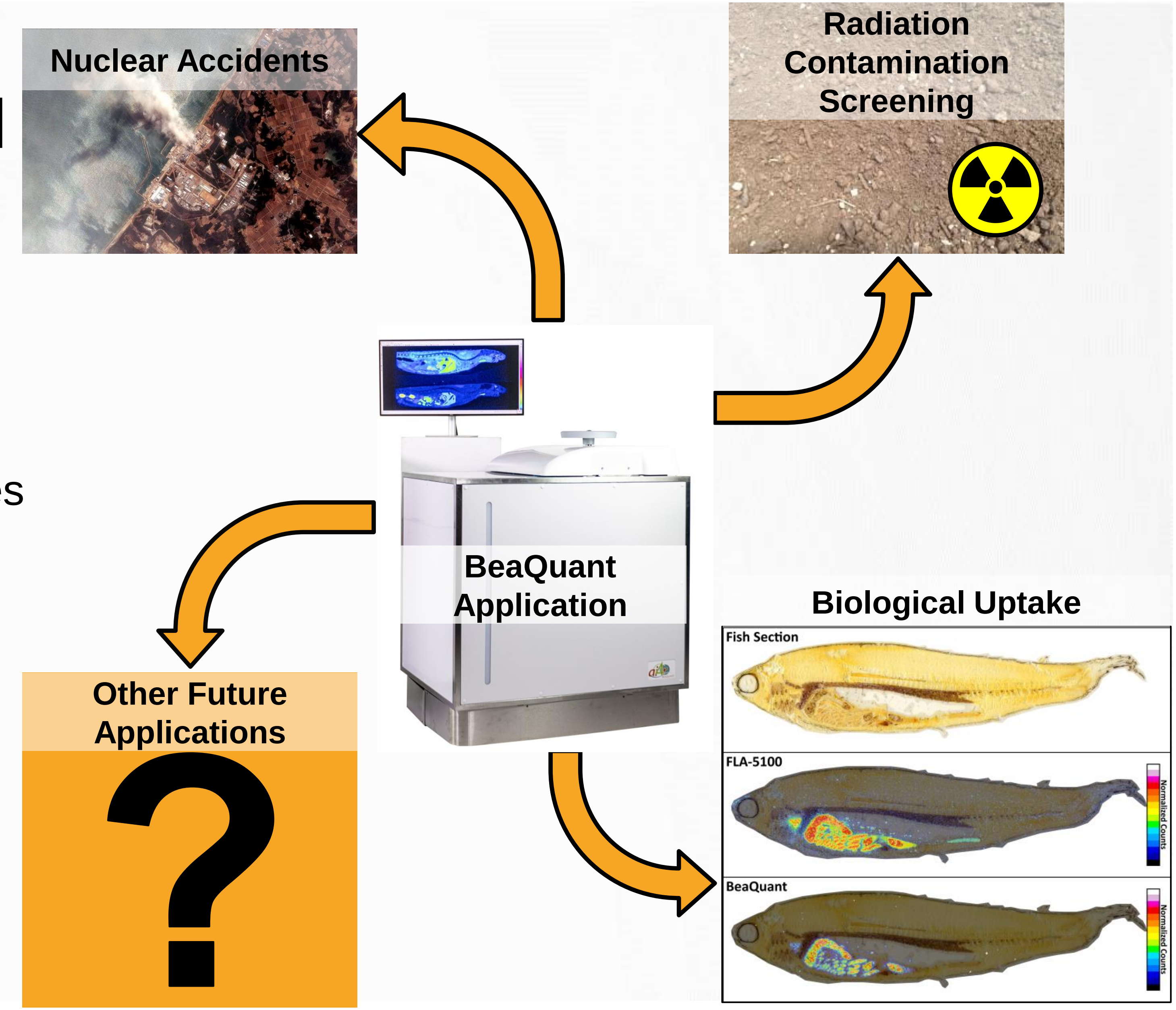

ACKNOWLEDGEMENTS

Singapore Nuclear Research and Safety Initiative

JENNY AND ANTTI WIHURI FOUNDATION

- Funders:
  - Singapore Nuclear Research & Safety Initiative
  - Jenny and Antti Wihuri Foundation
- Supervisors:
  - Gareth Law (Helsinki: Radionuclide Reaction and Fate)
  - Marja Siitari-Kauppi (Helsinki: Nuclear Waste Disposal)
- Collaborators:
  - Risto Koivula (Helsinki: Ion Exchange Group)
  - Team in AI4R (Collaborators from Nantes, France)
  - Joni Parkkonen (Collaborator from the University of Jyväskylä)

ai4r

UNIVERSITY OF JYVÄSKYLÄ

University of Helsinki, Radiochemistry Unit (taken in 2018)

ai4r, the company which commercialised BeaQuant™ (taken in 2022)